

X-ray emission from He-like $n = 2$ charge states produced in tokamak plasmas

E. Källne and J. Källne

Harvard-Smithsonian Astrophysical Observatory, Cambridge, Massachusetts 02138

A. K. Pradhan

Department of Physics, University of Windsor, Windsor, Ontario, Canada N9B 3P4,

(Received 13 August 1982)

Measurements of He-like x-ray line spectra for sulfur and chlorine impurity ions in the Alcator-C tokamak plasma are reported. Results are presented on the relative line ratios of the resonance (w), intercombination (x and y), and forbidden (z) lines as well as dielectronic satellite lines for plasma conditions of $T_e = 1.0\text{--}1.8$ keV and $N_e = (1.5\text{--}7) \times 10^{14}$ cm $^{-3}$. The results are compared with atomic calculations employing accurate atomic data which take into consideration effects on the line ratios due to collisional coupling between the $n = 2$ states involved.

I. INTRODUCTION

Characteristic x-ray emission has attracted attention as a means to diagnose hot plasmas be it from far away astronomical objects (supernova remnants, solar flares, etc.) or laboratory plasmas, i.e., inertially confined (exploding wires, laser-irradiated pellets, etc.) or magnetically (for instance, tokamak) confined discharges. Different wavelength regions of the emission spectra can be chosen to suit different purposes, and here we shall be concerned with the He-like spectrum of medium- Z elements (sulfur and chlorine). Ions in the helium isoelectronic sequence tend to remain, owing to the high excitation and ionization energies, in a plasma for comparatively longer time than ions in other sequences. Furthermore, the energy-level structure of the first few excited states of He-like ions is such that these states provide certain lines useful for diagnostics over extended ranges of electron temperature (T_e) and density (N_e). Also, from the point of view of atomic physics, the necessary atomic data required for such diagnostics are known to a fair degree of accuracy.

The principal He-like spectrum involving transitions from the $n = 2$ excited states is made up of the resonance (w), the intercombination (x and y), and the forbidden (z) transitions from the $1s2p$ states (2^1P_1 , 2^3P_2 , and 2^3P_1) and the metastable state $1s2s$ (2^3S_1), to the $1s^2$ ground state (1^1S_0); transitions are identified by letters in the conventional¹ way. In addition, dielectronic recombination leads to doubly excited Li-like ion states which give rise to $1s^22p$ - $1s2p^2$ satellites to the resonance transition; in particular, we are interested in the k line ($2^2P_{1/2}$ - $2^2D_{3/2}$).

Relative intensities of these lines can be interpreted on the basis of atomic models. The predicted line ratios depend crucially on the computed population rates for the excited $n = 2$ states which in turn reflect the plasma conditions in terms of T_e and N_e as well as the ionization balance of the element under study. Some of these rates are not known to desired accuracy, and this makes the plasma diagnostics correspondingly uncertain.

The present studies were performed at the Alcator-C tokamak² at the Massachusetts Institute of Technology (MIT). The plasma of this machine consisting of hydrogen, deuterium, or helium contains traces of sulfur and chlorine impurities from the vacuum vessel. The plasma is sustained for a duration of several hundred milliseconds, and unique for the Alcator-C tokamak is the high-density operation. Our measurements were performed in the density range $(1.5\text{--}7) \times 10^{14}$ cm $^{-3}$, which is a region of particular interest to study the importance of collisional effects in the population of the 2^3P and 2^3S states. Effects due to electron collisional mixing of the $n = 2$ metastable states have been studied in the He-like spectra of low- Z elements (for instance, oxygen and neon) provided by solar-flare observations.³ Here we present the first such study of higher- Z elements where the $J = 1$ and $J = 2$ fine-structure splitting of the 2^3P state is stronger and experimentally separable. Another unique feature of the present experiment is the high data-acquisition rate so that an extended x-ray spectrum of good statistical accuracy can be recorded for a single plasma discharge. This allows one, for instance, to compare spectra of discharges which

have been characterized to be constant on the basis of set external parameters and diagnosed main plasma parameters; i.e., we can explore whether this characterization of the plasma fully specifies the plasma conditions that determine the x-ray line emission.

The theory of line intensities from He-like ions was initially developed for solar diagnostics by Gabriel and Jordan.^{1,4} A number of calculations incorporating improved atomic data have since been carried out.^{1,5-7} Owing to the collisional depletion of the 2^3S state, resulting in enhancement of 2^3P populations, any ratio of two out of the three lines z , $(x+y)$, and w is expected to be density dependent; the largest such dependence being in the line-intensity ratio $R = z/(x+y)$. The electron density may be obtained from the observed R as follows:

$$N_e = N_c \left(\frac{R_0}{R} - 1 \right), \quad (1)$$

where R_0 is the low-density limit of R (no collisional coupling) and N_c is a characteristic density depending on atomic parameters for the given ion.^{5,8} Calculations⁴⁻⁷ in the coronal approximation have been done including atomic processes such as electron excitation with autoionizing resonances,^{9,10} cascades from higher levels, radiative and dielectronic recombinations, etc., and have been tested against He-like spectra of low- Z elements. Thus the available observations^{11,12} for C V, O VII, and Ne IX, both from laboratory and astrophysical sources, appear to be explicable even in the density regimes where collisional coupling amongst excited states considerably alters the line ratios from their low-density limit.

Initially, the temperature dependence of the lines from He-like ions was not fully appreciated since the $n=2$ states themselves have energy separations far less than their energy separation relative to the ground state. Therefore the main temperature dependence in the line intensities does not arise through the usual exponential factor $\exp(-\Delta E/T)$ inherent in the excitation rates. However, it has now been shown (e.g., Ref. 7) that the collision strengths, averaged over the electron distribution, for the triplet states behave in a similar manner with varying temperature, but it is quite different from that of the singlet states, and hence a line-intensity ratio such as $(x+y+z)/w = G$ varies significantly with temperature and has proved to be useful as temperature diagnostics. Another line-intensity ratio of interest in this work is $(x+y)/w = G/(1+R)$, which should be both density and temperature dependent. The ratio $(x+y)/w$ is expected to increase with increasing density (decreasing R) and with decreasing temperature (increasing G); G in-

creases rather sharply as T_e decreases below T_m , where T_m is the temperature of maximum abundance of the charge state considered. This is of relevance for the Alcator plasma where a deliberate increase in N_e results in decreased T_e and vice versa. Calculated values for $G(T)$ and $R_0(T)$ employing the most up to date atomic data are given elsewhere (see Sec. IV). In the present work we employ those values and compute new ones pertaining to the plasma conditions in the Alcator experiments.

The objective of the present paper is twofold. First, we wished to investigate the plasma diagnostics aspect of x-ray emission studies on the basis of our new results of measured line ratios compared with new calculations also presented here. Second, we hoped that by confronting calculated results with the measured line ratios obtained under partly known plasma conditions in a density regime not hitherto explored, we might shed light on questions of atomic processes in hot plasmas in general. The data presented here represent an expansion of the measurements published previously,¹³ and the accompanying analysis based on the theory presented in Refs. 8-10 was adapted to yield results for sulfur and chlorine.

II. EXPERIMENT

This experiment was carried out at the Alcator-C tokamak at MIT with a Bragg-crystal spectrometer. Access to the plasma was provided by a (5×20) -cm² view port which also accommodates a circular (16.5-cm-diameter) molybdenum limiter. The limiter defines the plasma spatially, but the radiation studied here comes from the plasma within a radius of 5-8 cm. The spectrometer was connected to the tokamak vacuum vessel through a reentry tube that placed the entrance slit of the spectrometer 53 cm from the plasma major radius. This distance was somewhat decreased compared with the configuration for previously reported measurements.¹³ A 0.05-mm-thick Be foil at the end of the reentry tube separated the two vacuums. The general layout of the experiment can be seen in Fig. 1(a).

The spectrometer is of the van Hamos geometry¹⁴ with a cylindrically bent (of radius 58.5 cm) crystal to provide focusing, and hence source imaging in one direction and diffraction in the other (horizontal) direction [see Fig. 1(b)]. The main elements of the instrument are the entrance slit (0.2-mm wide and 6-mm high), the pentaerythritol (PET) crystal (15×10 cm²), and a position-sensitive detector¹⁵ (active area 6×100 mm²). The slit-crystal and crystal-detector distances are 108 cm with the center lines forming an angle of $\theta_c = 113.0^\circ$; i.e., the Bragg angle is 33.5° in the center. High-efficiency diffraction

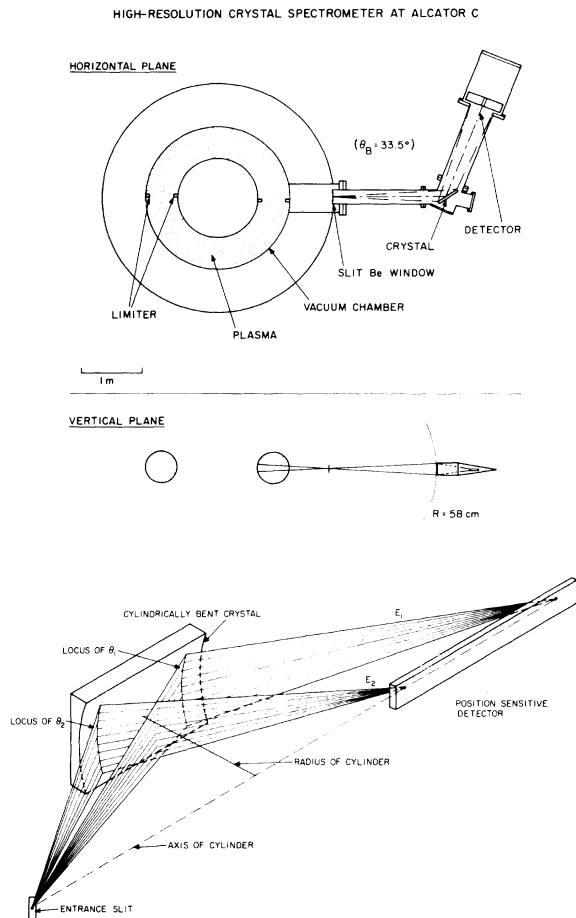


FIG. 1. Layout of the spectrometer at the Alcator-C tokamak (a) and the spectrometer geometry (b).

was obtained from the (002) plane of the PET crystal which has a lattice spacing of $2d = 8.742 \text{ \AA}$ at a nominal resolution of $\Delta\lambda/\lambda < 1/5000$. The effective wavelength band of the spectrometer is $\lambda = 4.3\text{--}5.3 \text{ \AA}$. Because of a mismatch between spectrometer and view-port apertures, we could simultaneously cover a bandwidth of $\Delta\lambda = 0.7 \text{ \AA}$. This was sufficient to fully cover the length of the detector. Different parts of the spectral range $4.3\text{--}5.3 \text{ \AA}$ were recorded by appropriately positioning the detector and by rotating (in the plane of the Bragg angle) the crystal.

So far we have not employed the imaging capability of the spectrometer. This simplified, among other things, the detector requirements so that we could use a commercially available single-wire proportional counter for one-dimensional recording of the x-ray spectra. The spatial resolution it provides, about $\leq 0.4 \text{ mm}$, full width at half maximum (FWHM), at $E_{h\nu} = 2.7 \text{ keV}$, is adequate in comparison to the total

observed line resolution of $\Delta\lambda/\lambda = 1/2000$ for ion temperatures of $T_i > 700 \text{ eV}$; the Doppler line broadening is $\Delta\lambda/\lambda \approx 1/3000$ at $T_i = 700 \text{ eV}$ for radiation of $\lambda = 4.4 \text{ \AA}$ from Cl ions. This resolution is retained for count rates up to the level of about $3 \times 10^4 \text{ s}^{-1}$.

This experiment was directed to the study of He-like line spectra for which calculations have given quite accurate wavelengths.¹⁶ We therefore used the well identified w and z lines (see below) as reference to fix wavelength scales in order to identify interjacent lines in the spectra of S and Cl. That the detector response is a linear function of position was verified in tests with 5.9-keV x rays from a ⁵⁵Fe line source.

Sulfur and chlorine appear as small amount impurities in the Alcator machine. The x-ray line intensities therefore reflect their abundance as well as the emissivity which both may vary with plasma conditions. Here we concentrate on relative line intensities, which are not subject to the abundance variation, for different plasma conditions as determined by macroscopic and diagnosed parameters. A typical Alcator plasma discharge in H₂, D₂, or He is characterized by a toroidal field of 60–100 kG and a plasma current of 100–600 kA. The steady current state lasts for about 200 ms. Information on the electron temperature T_e can be obtained from continuum (bremsstrahlung) x ray¹⁷ and electron cyclotron-radiation¹⁸ measurements. Typical discharges have temperatures in the range $T_e = 1\text{--}1.8 \text{ keV}$. The electron density and its time development are given for each discharge by interferometer measurements.¹⁹ The density is a parameter easily variable through adjustment of the gas injection. Here we studied x-ray spectra for steady-state central densities in the range $N_e = (1.5\text{--}7) \times 10^{14} \text{ cm}^{-3}$. The spectrometer views a 5-cm vertical portion of the central plasma core, and an electronics gate is used for time selection in the discharge.

III. RESULTS

A typical example of a measured x-ray spectrum from a single plasma discharge is shown in Fig. 2. The detector was in this case set to detect the He-like spectrum of Cl in which the principal lines w, x, y, and z are readily identified. The predicted relative positions of these lines agree with our observations. Moreover, three $n = 2$ satellites to the resonance line (q, r, and k) are also seen (for a discussion about these lines see Refs. 13 and 20) apart from some foothills on the long-wavelength side of w indicating higher $n \geq 3$ satellites. Except for k, the dielectronic recombination satellites are predict-

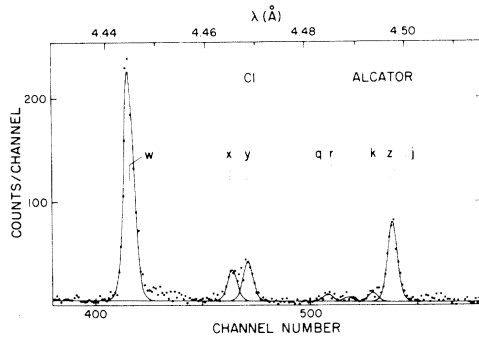


FIG. 2. Example of measured He-like spectrum for chlorine from a single plasma discharge characterized by $N_e \approx 3 \times 10^{14} \text{ cm}^{-3}$ and $T_e \approx 1.3 \text{ keV}$. Indicated line positions refer to the predictions of Ref. 16 and the curves shown represent a line fit to the data. Identified lines have been marked with letters in the conventional (Ref. 1) way:

- w, $1s^2 1S_0 - 1s 2p^1 P_1$; x, $1s^2 1S_0 - 1s 2p^3 P_2$;
 y, $1s^2 1S_0 - 1s 2p^3 P_1$; z, $1s^2 1S_0 - 1s 2s^3 S_1$;
 q, $1s^2 2s^2 S_{1/2} - 1s (2s 2p^1 P)^2 P_{3/2}$;
 r, $1s^2 2s^2 S_{1/2} - 1s (2s 2p^1 P)^2 P_{1/2}$;
 k, $1s^2 2p^2 P_{1/2} - 1s 2p^2 D_{3/2}$; j, $1s^2 2p^2 P_{3/2} - 1s 2p^2 D_{5/2}$.

ed^{1,16,20} to have wavelengths closer to the x, y, and z lines than is experimentally separable. From the predicted relative line-intensity ratios²⁰ and using k as a reference, we estimate that the satellite interference is insignificant except for the j satellite at 4.497 Å; for instance, some 15% of the z line for the conditions in Fig. 2 could actually come from the unresolved j satellite. The above discussion applies as

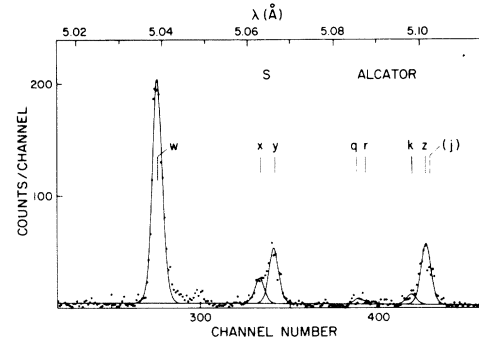


FIG. 3. Example of measured He-like spectrum for sulfur from a single plasma discharge characterized by $N_e = 3 \times 10^{14} \text{ cm}^{-3}$ and $T_e = 1.3 \text{ keV}$. Letter symbols and line positions have the same meaning as in Fig. 2. Curves shown represent a line fit to the data.

well to the He-like spectrum measured for sulfur, an example of which is shown in Fig. 3.

The measured line intensities for x, y, and z, which are always given relative to w unless stated otherwise, were obtained from line fits to the spectra with a nearly Gaussian shape of the width best fitting the w line; the uncertainties given are those of the standard deviations in the count statistics of each line. We first present typical average values which can be considered representative for discharges in the standard regime of the Alcator plasma parameters mentioned above. The results on such average relative line intensities of x, y, and z, and the ratios

$$G = (x + y + z)/w,$$

$$R = z/(x + y),$$

and x/y , based on data from some 15 runs each of 20–40 discharges are given in Table I. The data material has been extended since the previously reported results,¹³ especially for sulfur where some

TABLE I. Intensities of the lines x, y, and z relative to the resonance line w, and the line-intensity ratios $G = (x + y + z)/w$, $R = z/(x + y)$, and x/y . The experimental values are averages representing typical Alcator plasma conditions of $N_e \approx 3 \times 10^{14} \text{ cm}^{-3}$ and $T_e \approx 1.3 \text{ keV}$. Theoretical relative intensities for these conditions are also given.

Line-intensity ratios	Sulfur		Chlorine	
	Expt.	Theory	Expt.	Theory
x	0.16	0.15	0.17	0.16
y	0.29	0.29	0.25	0.24
z	0.41	0.34	0.39	0.43
G	0.85	0.78	0.81	0.83
R	0.97	0.77	1.04	1.08
x/y	0.55	0.52	0.69	0.65

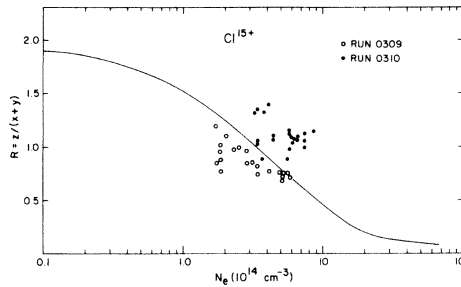


FIG. 4. Results for chlorine on the line-intensity ratio $R = z/(x + y)$ for individual plasma discharges plotted vs the electron density. Two sets of data are shown (distinguished by the symbols of open and filled circles) representing measurements of different days. Solid line is the calculated density dependence of R .

line-intensity ratios have changed.

An attempt to measure the correlation between the line-intensity ratio $R = z/(x + y)$ and the electron density gave the result shown in Fig. 4. Two sets of single-discharge data are presented representing measurements of two different days. The N_e values used here are interferometer measurements and represent the central peak value. The errors shown in this figure are statistical ones to which should be added the uncertainty of the j line admixture in the case of the z intensity given. If we were to correct for this admixture, as described above, R would be decreased by $(15 \pm 5)\%$. A systematic trend of decreasing R with increasing N_e can be dis-

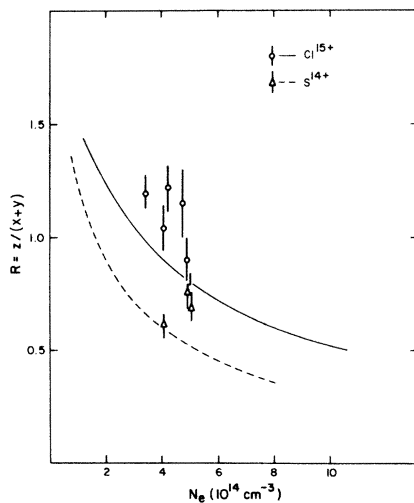


FIG. 5. Comparison of data on the line-intensity ratios $R = z/(x + y)$ for chlorine and sulfur. Discharges of similar densities were added. Solid line is the calculated density dependence of R .

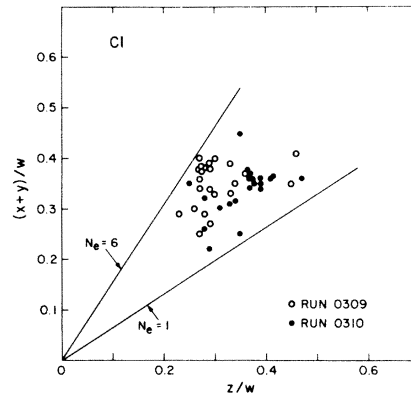


FIG. 6. Scatter plot of measured intensities for z and $(x + y)$ (relative to that of w) for the same sets of data shown in Fig. 4. Straight lines indicate the predicted bounds of variation of $(z, (x + y))$ for plasma densities in the range $(1-6) \times 10^{14} \text{ cm}^{-3}$ for an assumed product T_e of 1.2 keV.

cerned in each of the two sets of results. Another observation to make is the apparent difference of some 25% between the two days of measurements. No deliberate changes were made between these measurements except for routine tuning of the machine parameters. The data of each day also show a considerable scatter which is larger than can reasonably be referred to as statistical fluctuations. The data therefore seem to suggest that besides the $R(N_e)$ dependence there are variations that do not correlate with the electron density as measured. A comparison between R values measured for S and Cl over a limited N_e range can be found in Fig. 5.

A basic question for the interpretation of the N_e dependence of R is whether $R(N_e)$ is due to a redistribution of intensity between the z and the x and y . Figure 6 shows a plot of value pairs $(z, (x + y))$ of the same data sets as discussed before. The data show no apparent preference for an antilinear variation between z and $(x + y)$, but the largest variations tend to occur with the pattern of simultaneous increases/decreases in both z and $(x + y)$. However, the Alcator plasma does not allow the electron density to be varied independently of the electron temperature, the results on $z/(x + y)$ vs N_e do not represent constant T_e conditions. We can, however, attempt to reveal T_e -dependent effects in these data by inspecting for a correlation between $G = (x + y + z)/w$ and k/w . Both G and k/w are predicted to be T_e dependent so as to decrease with increasing T_e . Our results on the value pairs $(G, k/w)$ are shown in Fig. 7. We observe a variation of about $\pm 20\%$ around the average G of about 0.63 for these sets of data. There appears to be a

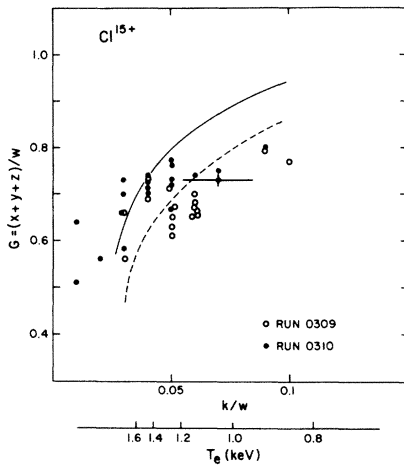


FIG. 7. Scatter plot of measured intensities for $G = (x + y + z)/w$ and k/w for the same sets of data shown in Fig. 4. Solid line is the predicted locus of $(G, k/w)$ based on calculations of the dependences of k/w (from Ref. 20) and G on temperature T_e , assuming a plasma in coronal equilibrium.

correlation between this variation and the k line intensity suggesting that a temperature dependence is at play here. The errors in k/w , however, are quite large for more quantitative conclusions to be drawn, but again it seems that we are encountering variations in G that are beyond the T_e dependence and that exceed the statistical standard deviations in the data points.

The unsystematic variations in G and R are denoted unsystematic since they can occur between discharges which would be judged to be similar on the basis of their parameter characterization. These variations, however, are not limited to the ratios G and R of the principal lines w , x , y , and z . In Fig. 8 we show examples of spectra from two discharges where the relative line intensities of x , y , or z markedly deviate from the typical averages for the series of shots considered. These variations are significantly larger than could be accounted for as sta-

tistical deviations, and variations of the order $\pm 50\%$ around the averages of x , y , and z relative to w have been recorded. Of particular interest is the ratio x/y which is expected not to depend on plasma conditions according to commonly used theories. The examples in Fig. 8 show x/y ratios which are both smaller and larger than the typical average; the numerical value for these cases is given in Table II. These examples were picked from a run consisting of 20 discharges of which some 20% showed x/y values that deviated from the mean value. This is a fairly high fraction since for other runs all x/y values are consistent with the average. It is also interesting to note that of some 50 runs and 2000 discharges measured, the x/y value for whole runs of discharges does not show much variation. Anomalous x/y ratios are observed for chlorine and sulfur alike. Furthermore, since these variations are not concurrent with any foreign line structure intensities in adjacent wavelength regions, they cannot be explained away as interference from other elements. With regard to the interference from other lines of the same element we note that dielectronic satellites have been predicted with wavelengths unseparately close to those of x and y . These, however, are predicted to be an order of magnitude weaker than k and can be estimated to be insignificant contributors in our spectra. Moreover, these satellites would be expected to vary along with the k satellite, and no correlation between the ratio x/y and the k line intensity has been seen. Finally, the observed positions of the x and y lines are constant. Thus the observed variations must be ascribed to the x and y line intensities.

IV. THEORETICAL COMPUTATIONS

In this section we theoretically evaluate and briefly describe typical features of the line-intensity—ratio parameters of interest. For the four main lines (w , x , y , and z) under consideration, these are R_0 , N_e , and G as a function of electron temperature. Recent calculations for a number of He-like ions have been carried out, and a study of the systematic variations correlated with temperature and

TABLE II. Results on the line-intensity ratios x/y , $G = (x + y + z)/w$, and $R = z/(x + y)$; two discharges of a day's run with extreme x/y ratios have been selected and compared with averages for the run.

Discharge identification number	x/y	R	G
10	1.24 ± 0.25	0.83 ± 0.12	0.71 ± 0.07
14	0.48 ± 0.05	0.93 ± 0.06	0.73 ± 0.04
Average	0.68	1.10	0.64

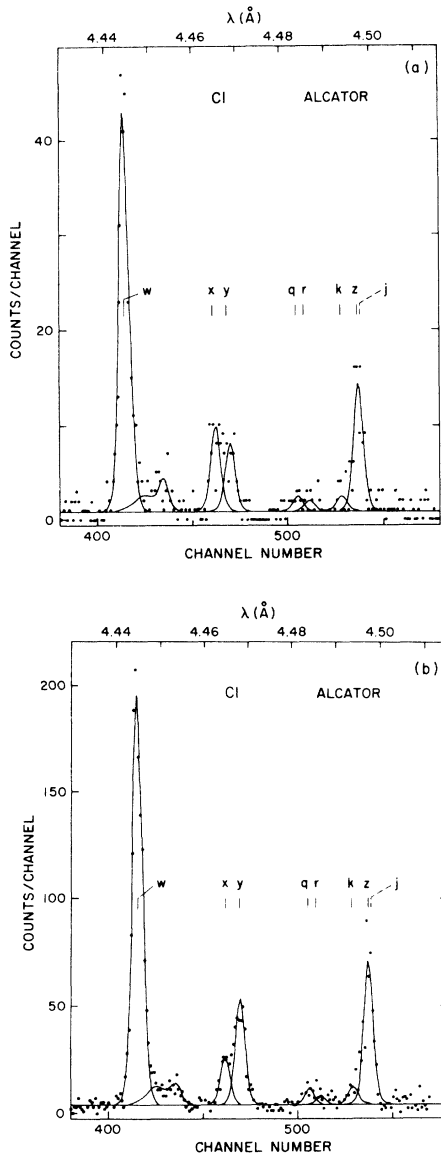


FIG. 8. Examples of measured He-like spectra for chlorine which show line-intensity ratios x/y that are (a) larger and (b) smaller than the typical average value.

nuclear charge has been made.^{7,8} The basic theoretical data for the analysis of present observations are taken from these studies, and new calculations were done for line-intensity ratios not included in earlier work. The forbidden to intercombination line-intensity ratio R is calculated from $R_0(T)$ and $N_e(T)$ as in previous works.

Since we are dealing with the intermediate—electron-density range, it is necessary to consider whether collisional redistribution amongst the $n=2$ states (other than the 2^3S to 2^3P ,

which is always included) might significantly affect the line-intensity ratios. An examination of the magnitude of the relative excitation rates reveals that the density dependence may also manifest itself through collisional transfer from the 2^1S_0 to the $2^{1,3}P$ states. The two-photon radiative-decay rate $1^1S_0-2^1S_0$ is $2.0 \times 10^8 \text{ s}^{-1}$ for S XV, and the calculated rate coefficients for electron- and proton-impact excitation of $2^1S_0 \rightarrow 2^1P_1$ are 2.58×10^{-9} and 1.80×10^{-9} , respectively (all rate coefficients in $\text{cm}^3 \text{sec}^{-1}$), at 0.9 keV and 2.62×10^{-9} and 3.80×10^{-9} at 1.7 keV. It should be noted that the proton excitation rate, to be discussed below, is much more temperature dependent and exceeds the electron excitation rate at the higher temperature. Thus contributions from 2^1S_0 to the 2^1P_1 level population are expected to be important at densities higher than 10^{16} cm^{-3} , i.e., outside the density range of the present experiment. The $2^1S_0 \rightarrow 2^3P_1$ excitation rate is lower; hence the mixing should occur at even higher densities. The line-intensity ratio G therefore depends only on temperature and not on density although the situation may be quite different in the densities higher than ours where G is both temperature and density dependent. Calculations of $G(T)$ were carried out for two cases, namely, a plasma in ionization equilibrium and for a purely ionizing plasma with no recombinations. The latter G values are lower than the former because recombinations contribute more to the triplet states than to the singlets.

Another useful line-intensity ratio for diagnostics is the intercombination to resonance line-intensity ratio, $(x+y)/w = G/(1+R)$ described earlier. Computed values R_0 for S XV and Cl XVI at $T_m \approx 1.3$ keV are 2.18 and 1.90, respectively. Along with $G(T_m)$, computed to be about 0.75, we obtain $(x+y)/w = 0.24$ and 0.26, respectively (within the coronal approximation), for the two ions. From the expressions given earlier it is seen that at $N_e = N_c$, the forbidden to intercombination line-intensity ratio falls to half its coronal value at the characteristic density for a He-like ion, i.e., $R = R_0/2$. This implies that $(x+y)/w$ at $N_e = N_c$ is 0.36 for S XV and 0.38 for Cl XVI where the densities N_c at T_m are computed to be $1.8 \times 10^{14} \text{ cm}^{-3}$ and $3.6 \times 10^{14} \text{ cm}^{-3}$, respectively. These line-intensity ratios at the characteristic densities lie in the middle of the present range of measurements, i.e., at plasma densities $(2-4) \times 10^{14} \text{ cm}^{-3}$.

The line-intensity ratio $R = z/(x+y)$ depends on the density through the relation

$$R = R_0 \left[\frac{1}{1 + \frac{N_e}{N_c}} \right]. \quad (2)$$

The density dependence

$$\left. \frac{dR}{dN_e} \right|_{N_e=N_c} = -\frac{R_0}{4N_c} \quad (3)$$

varies through the isoelectronic sequence because the ratio R_0/N_c decreases systematically with increasing atomic number Z . Subsequently, the density dependence, which is readily observable in solar data for oxygen and neon,³ becomes experimentally harder to detect for higher- Z elements.

The present experiment raises the question about variations in the relative intensities of the fine-structure lines x and y . The two lines x and y belong to the $J=2$ and $J=1$ fine-structure components of the 2^3P state, which decay to the 1^1S ground state by magnetic quadrupole ($M2$) and spin-forbidden electric dipole ($E1$) transitions, respectively, the latter being affected by Z -dependent mixing with the 2^1P_1 state. These transition rates are known from atomic calculations. Given the decay rates and assuming statistically weighted excitation rates (principally through electron-impact excitation of the ground state), one arrives at the expression

$$\frac{x}{y} = \frac{\frac{5}{9} \frac{A(2^3P_2 \rightarrow 1^1S_0)}{A(2^3P_2 \rightarrow 1^1S_0) + A(2^3P_2 \rightarrow 2^3S_1)}}{\frac{1}{3} \frac{A(2^3P_1 \rightarrow 1^1S_0)}{A(2^3P_1 \rightarrow 1^1S_0) + A(2^3P_1 \rightarrow 2^3S_1)}} \quad (4)$$

The coronal and Boltzmann (CB) limits for x/y are the same, i.e., 0.52 for SXV and 0.65 for Cl XVI, with no predicted dependence on plasma conditions within the standard framework of theoretical assumptions. Comparison can be made with a similar situation for H-like ions where the line-intensity ratio $(1s_{1/2}-2p_{1/2})/(1s_{1/2}-2p_{3/2})$ is expected to be 0.5 in the CB limits. However, Vinogradov *et al.*²¹ have shown that this ratio could increase up to 2 or more, in between the two limits, mainly owing to the effect of proton-impact excitation which preferentially populates the $2p_{1/2}$ state. It is known¹¹ that provided the transition energy $\Delta E \ll T_e$, proton excitation may well dominate electron excitation in causing transitions between closely spaced atomic levels; however, it depends critically on ΔE . In the H-like case, for $Z=10-20$, the ratio of the Lamb shift to the fine-structure energy splitting is $\sim 1/30$, hence the considerable preference for the $2p_{1/2}$ over the $2p_{3/2}$ in proton excitation from $2s_{1/2}$. We apply the theory of Vinogradov *et al.*²¹ to the ratio x/y in He-like ions and consider preferential excitation from the 2^3S_1 state to the 2^3P_1 over the 2^3P_2 . It is

permissible to ignore excitations from the 2^1S_0 state which, according to our calculations, do not contribute significantly at the densities of interest. Computing proton-impact excitation rates according to the theory of Vinogradov *et al.* and using electron-impact excitation rates by Pradhan *et al.*,¹⁰ we find for SXV that x/y could decrease to a minimum of about $x/y \simeq 0.45$ from its limiting value of 0.52. The relatively smaller proton mixing in the He-like case is owing to the fact that the transition-energy ratio is only about $\frac{1}{2}$ instead of $\frac{1}{30}$ as in the H-like case. The transition regions, from the coronal limit to $(x/y)_{\min}$ and back to the Boltzmann limit (where all population distributions are according to statistical weights), correspond to densities of $10^{13}-10^{14} \text{ cm}^{-3}$ and $10^{19}-10^{20} \text{ cm}^{-3}$, respectively, for SXV. There could be a further decrease in x/y , also owing to proton collisions, from deexcitation of 2^3P_2 to 2^3P_1 and from excitation of 2^1S_0 to 2^3P_1 . However, at the densities under consideration these two components would be very small.²² Thus the mentioned nonstatistical proton mixing effects could account for a 10–15% decrease in $(x/y)_{\text{CB}}$, and the variation would be density dependent. The effects of these atomic processes under equilibrium conditions are far too small to explain the observed magnitude of variations in x/y , let alone the fact they do not account for any enhancement.

V. DISCUSSION

The density regime of the present experiment is of particular interest for the possibility it offers to investigate collisional coupling of long-lived (metastable) excited states. The comparison between our data on the line-intensity ratio $R = z/(x+y)$ and calculations is shown in Fig. 4 and Table I. For densities in the range $(1.5-7) \times 10^{14} \text{ cm}^{-3}$ the observed R values are approximately reproduced by the calculation. We note that the R value here is reduced by a factor of 2–3 as compared with the ratio $R = R_0$ where collisional coupling between the 2^3S and 2^3P states is negligible. Unfortunately, there are no other data on S and Cl for the low-density regime to compare with our results. Other tokamak measurements have been made, however, for higher- Z elements, viz., measurements on Fe done at Princeton Large Torus (PLT)²³ at $N_e < 4 \times 10^{13} \text{ cm}^{-3}$ compared with $N_e \simeq 7 \times 10^{17} \text{ cm}^{-3}$. The predicted value for $R_0(\text{Fe})$ by Pradhan and Shull⁷ undershoots the PLT data of Bitter *et al.* by about 25%, but this is mainly owing to the fact that the calculations did not include intermediate-coupling effects which begin to manifest themselves significantly at about $Z > 20$. On the other hand, recent observations of He-like calcium²⁴ from low-density solar flares yield

a R_0 value very close to the predicted value, and very good agreement with the calculations of Pradhan *et al.*¹⁰ is found for the other ratios of w , x , y , and z as well. This, together with the good agreement between theory and observations for low- Z elements (up to neon), suggests that the calculations provide fairly accurate predictions for line-intensity ratios up to about $Z=20$; the problem encountered for higher- Z elements is owing to relativistic effects, for which calculations are now in progress for up to $Z=42$. We can thus interpret our results $R < R_0$ for S XV and Cl XVI as being a manifestation of the density effect.

Our data on the line-intensity ratio $R = z/(x + y)$ span the density range $(1.5-7) \times 10^{14} \text{ cm}^{-3}$, over which region R is predicted to vary by a factor of 2. Although there is a definite trend in data that R decreases with increasing N_e , there is also a significant scatter of the data points outside the predicted curve of $R = R(N_e)$. This impedes upon drawing quantitative conclusions from our $R = R(N_e)$ measurement. The same is true if one compares the R values for S and Cl (Fig. 5). For a density of about $3 \times 10^{14} \text{ cm}^{-3}$, the R value for Cl is predicted to be some 30% larger than for S.¹ The data shown in Fig. 5 show a difference in the same direction, but the significance of this result must be weighed against the scatter in R values. The measured average of R is about 10% smaller for S than for Cl (Table I).

The above comparison between measured and predicted R values has revealed quite an encouraging agreement between experiment and theory. With regard to the origin of the N_e dependence, however, the theoretical interpretation rests on the assumption of collisional coupling between the 2^3S_1 and $2^3P_{2,1}$ states. This means that while R is predicted to change $\pm 30\%$ over our N_e range, the change is only $\pm 15\%$ in z and $\mp 15\%$ in $(x + y)$. The final test of the theory would then be the observation of the correlated change $\Delta(z) = -\Delta((x + y))$. This, however, requires first of all data of good statistics to see the smaller variations. Second, one has to make sure that the plasma discharges, for which the z and $(x + y)$ line intensities were measured, were constant with regard to parameters other than N_e . In our case, for instance, the electron density is not independently variable from the electron temperature. Therefore our present data are not well suited to examine the explicit N_e -dependent correlation between z and $(x + y)$ since these line intensities are expected to vary with T_e as well.

In order to display temperature-dependent effects in line intensities, we turn to the ratios $k_r = k/w$ and

$$G = (x + y + z)/w .$$

Our data (Fig. 6) do indicate a correlation between

these parameters which at least to its trend resembles that given by the calculated dependencies of k/w and G on temperature T_e . We know from other diagnostic measurements that the typical temperature range of the Alcator plasma is $1 \leq T_e \leq 2$ keV (as indicated by the parameter k/w). Over this temperature range, G is predicted to vary some 50% which is the range of variation that we observe experimentally.

Among the parameters entering into the computation of G are the ionization-balance fractions that multiply the radiative and dielectronic recombination terms which contribute much more to the population of the triplet states than the singlet states. Therefore the observed ratio G also proves to be an indicator of the departure from ionization equilibrium; at least one such case^{7,25} is believed to be the astrophysical observations of the supernova remnant Puppis A. Although the tokamak plasmas are expected to be in a more or less steady-state situation, it has been experimentally¹² shown that there is a radial inward diffusion of the heavy ions that affects the ionization balance in the plasma. The effect of such diffusion in the present calculations would be to yield values of $G(T_e)$ lying somewhat away from the ionization equilibrium curve towards the G values obtained under the assumption of pure ionization (lower dashed curve in Fig. 7). We did not explicitly include the diffusion effect in our calculations since the observational scatter in the data exceeds the variations that might thus be produced.

The line-intensity ratio x/y has not been designated for any special plasma diagnostic use since this ratio is not expected to depend on the plasma conditions. Experimentally, we find that most plasma discharges show x/y ratios that are consistent with the predicted x/y ratios of 0.52 and 0.65 for S and Cl. The average values determined over many discharges are 0.55 and 0.69 for S and Cl which is a result in close agreement with theory. We also observe, however, discharges for which the x/y ratio deviates from the average. These variations should manifest changes in the population rates of the $2^3P_{1,2}$ states which in turn must reflect changes in plasma conditions. We have searched for possible correlations between the x/y ratio and the main plasma parameters such as N_e and T_e , but any obvious systematics of this kind have not been found. For instance, the example of extreme x/y values given in Fig. 8 and Table II represents discharges of similar properties as far as characterized by measurements of N_e and T_e ; parameters such as plasma current, gas, and toroidal magnetic field were also the same. Therefore if we assume that the N_e and T_e values are representative for the whole plasma ring, the x/y ratio must depend on other unmea-

sured features of the plasma.

In analogy with the suggested importance of collisional coupling (preferentially through protons) of the excited $2^2S_{1/2}$ and $2^2P_{1/2,3/2}$ states of H-like ions, the He-like $2^3P_{1,2}$ states could similarly be coupled to the metastable 2^3S state. The x/y ratio would then be sensitive to the proton density. However, the average ion charge for the Alcator plasma is generally small, $Z_{\text{eff}} < 1.5$, so that $N_e \simeq N_p$; a correlation between x/y and N_e ($=N_p$) is not suggested by our data.

One parameter which is not well monitored is the density (N_0) of neutrals (i.e., hydrogen or deuterium atoms) in the center of the plasma. It is generally believed that N_0/N_e is of the order 10^{-6} , so that the charge-exchange cross sections (for neutral ions on H-like ions) must be correspondingly larger than those of electron-impact excitation of the He-like ground state to be important. Therefore calculations are needed to assess if charge exchange could be the ghost-population mechanism affecting the x/y line-intensity ratio. In any case it seems to us that the observed peculiar variations in x/y call for calculations that include a new population mechanism for the triplet 2^3P state which must then consider J -dependent effects.

Here we have called particular attention to the variations in the ratio x/y because they are experimentally quite conspicuous and interpretationally the most puzzling ones. Other variations occur in the x , y , and z lines relative to w ; there is also a scatter in the ratios G and R . Although some new excitation mechanisms might be required to explain these observations, one could possibly invoke some simpler explanations such as departure from coronal equilibrium conditions affecting the relative importance of excitation and recombination effects. Although the tokamak plasma is fairly well diagnosed, there remain open questions pertaining to the radial distribution of different charge states of the impurity ions. A related question pertains to the transport of impurities in the plasma, the source of the impurities, and the different local properties of the plasma. Therefore the possibility exists that the parameters of the plasma region yielding the x-ray emission observed is not always represented by the parameters measured. Such effects could at least provide a partial explanation of observed variations. Other possibilities are inhomogeneities in the plasma

because of stationary instability islands around the limiter.

VI. CONCLUSIONS

We have presented results of measurements of the He-like spectrum of S and Cl produced in the plasma of the Alcator-C tokamak. Calculations were performed in order to obtain predicted line intensities as a function of T_e and N_e over the ranges $T_e = 1-1.6$ keV and $N_e = (1.5-7) \times 10^{14}$ cm $^{-3}$ of experimental observations. Our single-discharge data show a systematic variation in the intensity ratio of the forbidden to intercombination, $R = z/(x+y)$, which can be ascribed to the calculated N_e dependence. This observation verifies the predicted collisional (N_e -dependent) population transfer 3S to 3P . For the plasma conditions of a typically average Alcator discharge ($N_e \simeq 3 \times 10^{14}$ cm $^{-3}$ and $T_e \simeq 1.2$ keV), the R value is predicted to have decreased by about 50% for S and Cl as compared to R_0 in the low-density limit of no collisional effects. Our observed average value for R as the values of intensities of x , y , and z relative to the resonance line w are close to the calculated ones. The agreement found between theory and experiment, with regard to N_e dependence and average line intensities, supports the model and the atomic rates of the calculations. However, our single-discharge measurements show line-intensity-ratio variations which appear uncorrelated to any known changes in the plasma conditions. In particular, the x/y line-intensity ratio is observed to vary by up to 50% from its average value which is the observed value for most discharges. A varying x/y ratio would require an atomic process that selectively affects the population of the $^3P_{2,1}$ states as compared to the customary ones which are determined by statistical weights. The observation of unsystematic intensity variations of the He-like principal lines also seems to suggest that the main plasma parameters and machine parameters do not fully specify the plasma conditions affecting the x-ray line emission in the plasma core.

ACKNOWLEDGMENTS

It is a pleasure to acknowledge the cooperation and support from Dr. R. Parker and the Alcator group. This work was supported by the U.S. Department of Energy and by the National Sciences and Engineering Research Council of Canada.

¹A. H. Gabriel, Mon. Not. R. Astron. Soc. **160**, 99 (1972).

²S. Fairfax *et al.*, in *Plasma Physics and Controlled Nuclear Fusion Research, Proceedings of the Eighth Inter-*

national Conference, Brussels 1980 (IAEA, Vienna, 1981), Vol. I, p. 439.

³G. A. Doschek *et al.*, *Astrophys. J.* **249**, 372 (1981).

⁴A. H. Gabriel and C. Jordan, Mon. Not. R. Astron. Soc.

- 145, 241 (1969).
- ⁵G. R. Blumenthal, G. W. F. Drake, and W. H. Tucker, *Astrophys. J.* 172, 205 (1972).
- ⁶R. Mewe and J. Schrijver, *Astron. Astrophys.* 65, 99 (1978).
- ⁷A. K. Pradhan and J. M. Shull, *Astrophys. J.* 249, 821 (1981).
- ⁸A. K. Pradhan, *Astrophys. J.* 263, 821 (1982).
- ⁹A. K. Pradhan, D. W. Norcross, and D. G. Hummer, *Phys. Rev. A* 23, 619 (1981).
- ¹⁰A. K. Pradhan, D. W. Norcross, and D. G. Hummer, *Astrophys. J.* 246, 1031 (1981).
- ¹¹D. L. McKenzie and P. B. Landecker, *Astrophys. J.* 259, 372 (1982).
- ¹²TFR Group, J. G. Doyle, and J. L. Schwob, *J. Phys. B* 15, 813 (1982).
- ¹³E. Källne, J. Källne, and J. E. Rice, *Phys. Rev. Lett.* 49, 330 (1982).
- ¹⁴L. van Hamos, *Ann. Phys. (Leipzig)* 17, 716 (1933); C. B. van den Berg and H. Brinkman, *Physica (Utrecht)* 21, 85 (1955); H. W. Schnopper and P. O. Taylor, U.S. Department of Energy Report No. E4-76-S-02-4021 (unpublished).
- ¹⁵C. J. Borkowski and M. K. Kopp, *Rev. Sci. Instrum.* 46, 951 (1975).
- ¹⁶U. I. Safronova, *Phys. Scr.* 23, 241 (1981); L. A. Vainshtein and U. I. Safronova, *At. Data Nucl. Data Tables* 21, 49 (1978).
- ¹⁷J. E. Rice, K. Molvig, and H. I. Helava, *Phys. Rev. A* 25, 1645 (1982).
- ¹⁸I. H. Hutchinson and S. E. Kissel, *Phys. Fluids* 23, 1698 (1980).
- ¹⁹S. M. Wolfe, K. J. Button, J. Waldman, and D. R. Cohn, *Appl. Opt.* 15, 2645 (1976).
- ²⁰C. P. Bhalla, A. H. Gabriel, and L. P. Presnyakov, *Mon. Not. R. Astron. Soc.* 172, 359 (1975).
- ²¹A. V. Vinogradov, I. Yu Skobelev, and E. A. Yukov, *Fiz. Plazmy* 2, No. 3, (1977) [*Sov. J. Plasma Phys.* 3, 389 (1977)].
- ²²M. J. Seaton, *Mon. Not. R. Astron. Soc.* 127, 191 (1964).
- ²³M. Bitter *et al.*, *Phys. Rev. Lett.* 43, 129 (1979).
- ²⁴C. Jordan and N. J. Veck, *Sol. Phys.* 78, 125 (1982); G. Doschek (private communication).
- ²⁵P. F. Winkler, C. R. Canizares, G. W. Clark, T. M. Markert, K. Kalata, and H. W. Schnopper, *Astrophys. J.* 246, L27 (1981).